RESEARCH ARTICLE

Histogram analysis of laser speckle contrast image for cerebral blood flow monitoring

Arkady S. ABDURASHITOV (✉)[1], Vladislav V. LYCHAGOV[1], Olga A. SINDEEVA[1], Oxana V. SEMYACHKINA-GLUSHKOVSKAYA[1], Valery V. TUCHIN[1,2,3]

1 National Research Saratov State University, Saratov 410012, Russia
2 Institute of Precise Mechanics and Control RAS, Saratov 410028, Russia
3 Interdisciplinary Laboratory of Biophotonics, National Research Tomsk State University, Tomsk 634050, Russia

Abstract Laser speckle contrast imaging (LSCI) is a powerful tool for blood flow mapping. In this paper, we described a simple algorithm based on histogram analysis of laser speckle contrast image to provide rapid differentiation between macro- and microcirculations. The algorithm was successfully verified by the study of blood flow in rat cortex under functional activation.

Keywords laser speckle contrast imaging (LSCI), histogram analysis, cerebral blood flow (CBF), rat

1 Introduction

Laser speckle contrast imaging (LSCI) is a powerful and easy-to-use method for blood flow mapping, especially in semi-transparent tissues. For this reason, this technique was first used to visualize retinal blood flow [1]. Although LSCI can be used for tissues possessing high scattering properties such as skin, the most impressive results are achieved with tissues having weak scattering properties. To date, LSCI has been actively used in cerebral blood flow (CBF) mapping [2–4] and intraoperative control in neurosurgery [5]. Laser Doppler flowmetry (LDF) is physically similar to LSCI [6] and essentially used for spatially-integrated blood flow measurements. Although modifications of scanning LDF are known, their temporal and spatial resolutions are limited by the scanning system capability [7]. Compared with LDF, LSCI can provide non-scanning full-field imaging of a relatively wide area of an object with a passable resolution.

Monitoring of skin perfusion is important for diagnosis

and therapy of some diseases. For instance, Huang et al. [8] proposed LSCI as a tool to estimate efficiency of laser treatment for nevus flammeus. Moreover, LSCI is also applied to visualize retinal blood flow [1,9]. In these applications, Tamaki et al. [9] developed the algorithm they called "normalized blur", in this method, ratio of the mean speckle intensity to difference between the mean speckle intensity and the instant speckle intensity is calculated. Another application of LSCI in the retina is for the study of retinal blood flow changes under functional activation using pharmacological agents [10].

LSCI was introduced initially as noninvasive method for CBF imaging; however, this technique requires optical clear [11] of a skin tissue and a part of the skull is removed to attain a direct access to the cortex [2,12]. LSCI is often combined with other methods such as multispectral reflectance imaging [13], fluorescence imaging of nicotinamide adenine dinucleotide in its reduced form (NADH) and flavoproteins [7], or used independently [14].

Another possible implementation of LSCI is to study depolarization wave propagation in the cortex [15], which is the main mechanism of migraine headache. In these studies, LDF was adopted for quantitative measurements of blood flow in a specific location of the cortex and LSCI was used for spatial mapping of the changes of CBF induced by the propagation of depolarization wave [7].

LDF has been the most common tool for CBF measurements with essentially point-wise access. Although magnetic resonance imaging and positron emission tomography can be also used to perform such monitoring, disadvantages of these techniques include low spatial resolution, contrast agents usage, ionizing radiation, and high cost of service [16]. By comparison, LSCI is a low-cost and high-performance imaging technique [17]. However, quantitative measurements using LSCI is very

complicated and still need improvements, particularly with regard to multiple scattering [4,18,19], sensitivity to light polarization [7,20], and velocity distribution of the particles [21,22]. To solve these problems partially, calibration on tissue phantom with known parameters [23] or multi-exposure LSCI [24] can be used. In spite of these efforts, LSCI is most widely used for relative measurements [2–4,7], rather than quantitative studies.

The estimated optical resolution of our LSCI system is approximately 120 µm, and typical size of cerebral blood vessels varies in the range from 5 to 500 µm. Obviously, optical resolution of this imaging system is not high enough to distinguish most of the vessels in microcirculatory bed. Although a single capillary, arteriole, or venule cannot be resolved in a speckle image, extracting information on microcirculatory bed is possible through analysis of contrast distribution within the portion of the speckle image that corresponds to unresolved images of these small vessels [4,25].

The common method for retrieving information from a speckle contrast image is based on region of interest (ROI) analysis. A few ROIs are usually selected in a speckle contrast image. Typically, one ROI is set to represent the vein of macrocirculation and another ROI represents the microcirculatory network [4,25]. Further processing is performed usually to calculate the average contrast value over the entire ROI. Much of the information on blood flow within the analyzed region is unused because of such averaging. Instead of adopting the ROI method, we proposed a simple technique to retain this additional information using histogram analysis of speckle contrast distribution. We attempted to enhance the capabilities of LSCI to perform qualitative measurements by describing a simple algorithm based on histogram analysis of an image obtain by LSCI to provide rapid differentiation of macro- and microcirculation.

2   Speckle image analysis

Typical speckle contrast image of a rat cortex is shown in Fig. 1. This image is obtained with the following setup: He–Ne laser working at 632.8 nm was used to illuminate the rat cortex; complementary metal-oxide-semiconductor (CMOS)-camera Basler acA2500-14 gm with 2.2 µm × 2.2 µm pixel size was adopted for image acquisition; imaging lens Computar M1614-MP2 is at f/6; speckle/pixel size ratio is approximately 9; spatial speckle contrast distribution was calculated using 7×7 pixels sliding window; 50 consecutive frames of raw speckle image were averaged into the single speckle contrast image; and frame rate of initial raw data is equal to 40 frames per second.

In this work, spatial speckle contrast distribution was calculated using the standard equation:
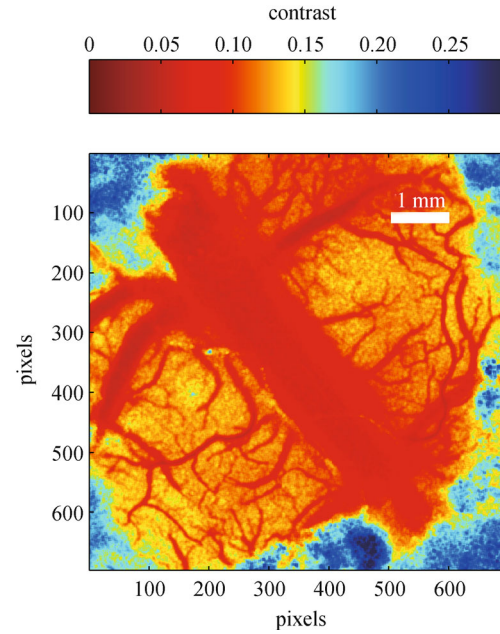

Fig. 1   Typical speckle contrast image

$$K = \frac{\sigma}{\langle I \rangle}, \tag{1}$$

where $\langle I \rangle$ is the mean value and σ is the standard deviation of intensity in the analyzed region of the raw speckle image. To reduce processing time, parallel computing and digital image processing were implemented [26]. Using these approaches, spatial speckle contrast analysis is described. Spatial distribution of the mean intensity $\langle I \rangle$ is given as convolution of the raw speckle image $IRaw$ with the $N \times N$ kernel matrix K of ones [27].

$$\langle I \rangle = \frac{1}{N^2}(IRaw*K). \tag{2}$$

Array of the standard deviation σ can also be expressed as [27]

$$\sigma = \frac{\sqrt{\dfrac{1}{N^2-1}\left[IRaw^2 * K - \dfrac{(IRaw*K)^2}{N^2}\right]}}{\dfrac{IRaw*K}{N^2}}. \tag{3}$$

In that case, the resulting speckle contrast map can be effectively calculated by vectorization of Eq. (1).

Further processing is devoted to differentiation of blood flow between macro- and microlevels. In this work, we employed histogram analysis of the speckle contrast image [26] to achieve rapid integral multiscale analysis of blood flow. We selected three ROIs in the speckle contrast image, as depicted in Fig. 2. Each ROI represents a vascular bed with different scale. The first ROI (ROI1) contains both large and small vessels. As shown in the speckle contrast
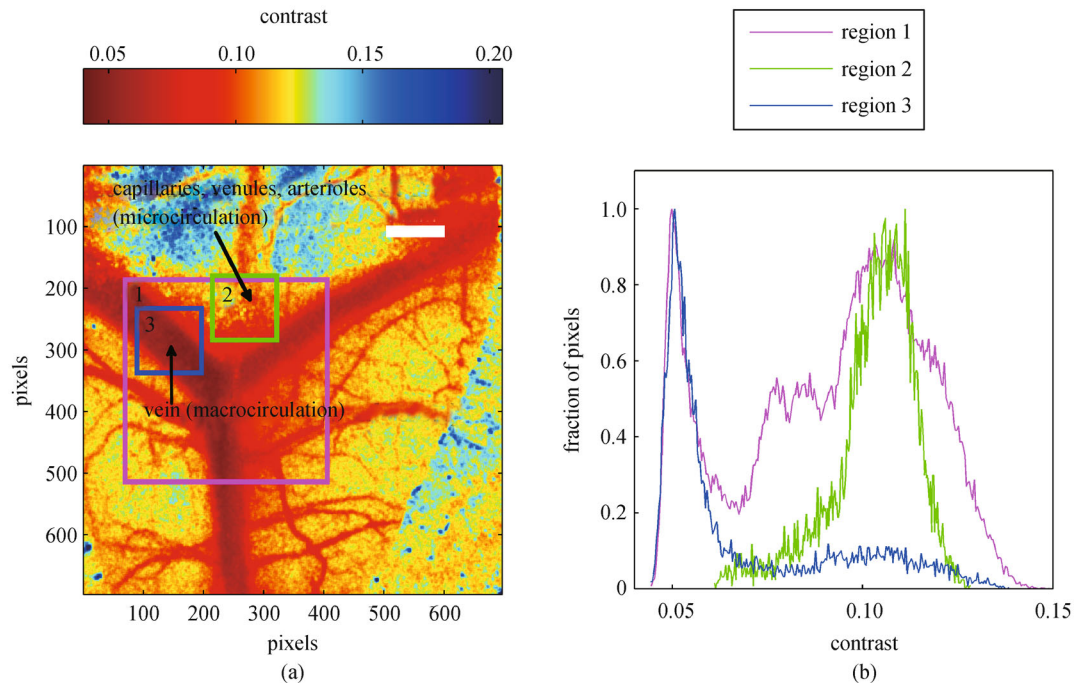
Fig. 2   Histogram analysis of speckle image. (a) Multiple ROIs in speckle contrast image; (b) normalized histograms of these ROIs

map, the distributions of blood flow in these both vessels are different. Results from the histogram analysis of laser speckle contrast image of this ROI showed two patterns of blood flow distribution, which were attributed to large (left side mode) and small (right side mode) vessels, respectively (see the purple curve in Fig. 2(b)). To validate this assumption, we constructed two additional small-sized ROIs: the second one (ROI2) corresponds to small optically unresolved vessels and the third ROI (ROI3) was a region with large vessels (as shown in Fig. 2(a)). The respective histograms of ROI2 and ROI3 coincide well with that of the ROI1 (Fig. 2(b)). A combination of histograms of the small-sized ROIs gives an expected bimodal distribution. In addition, the histogram of ROI1 contains some additional side modes corresponding to relatively large resolvable vessels on each side of the main trunk.

Thus, histogram analysis can provide integral rating of the speckle contrast image as a whole. However, information on some vessels can be lost and implicated because of unreasonably large ROIs.

During the experiment, changes of these modes with time can be tracked, including their relative and absolute positions, shape, and magnitude. According to the proposed concept, relative changes of these modes provide information on rearrangement of blood flow between macro- and microcirculatory network.

The main steps of the algorithm are as follows:

1) Constructing ROI that covers large vessels and adjacent microvascular bed;

2) Calculating histogram of this ROI;

3) Retrieving the modes of distribution and their parameters.

In the case of time lapse measurements of laser speckle contrast image, some artifacts can be caused by the motion of the sample. As a result of this sample motion, the pre-selected ROI (green block in Fig. 3) is not always in a desirable position. To resolve this issue, we improved the algorithm using correlation-based motion tracker. We selected a ROI to track and calculate cross-correlation of each speckle contrast image in time series with this region, as depicted in Fig. 4. Then, a peak value in each spatial cross-correlation function was found, and the position of this peak defines new coordinates of the ROI according to current image. Finally, a new ROI within each frame of the time series was constructed with respect to their own new coordinates (purple block in Fig. 3). Moreover, the selected region must have a well-recognizable structure (large vessels or network of small vessels) for cross-correlation procedure.

Results of time lapse measurements performed with statically overlaid ROI and with correlation-based motion tracker are presented in Fig. 5. The motion tracker can compensate the most part of artificial movements, and by using this tracker, the problem of exiting the vessels out of ROI can be avoided.

3   Experiment with animals

We mapped changes of CBF in hypertensive rats for differentiation of macro- and microcirculation. Hyperten-
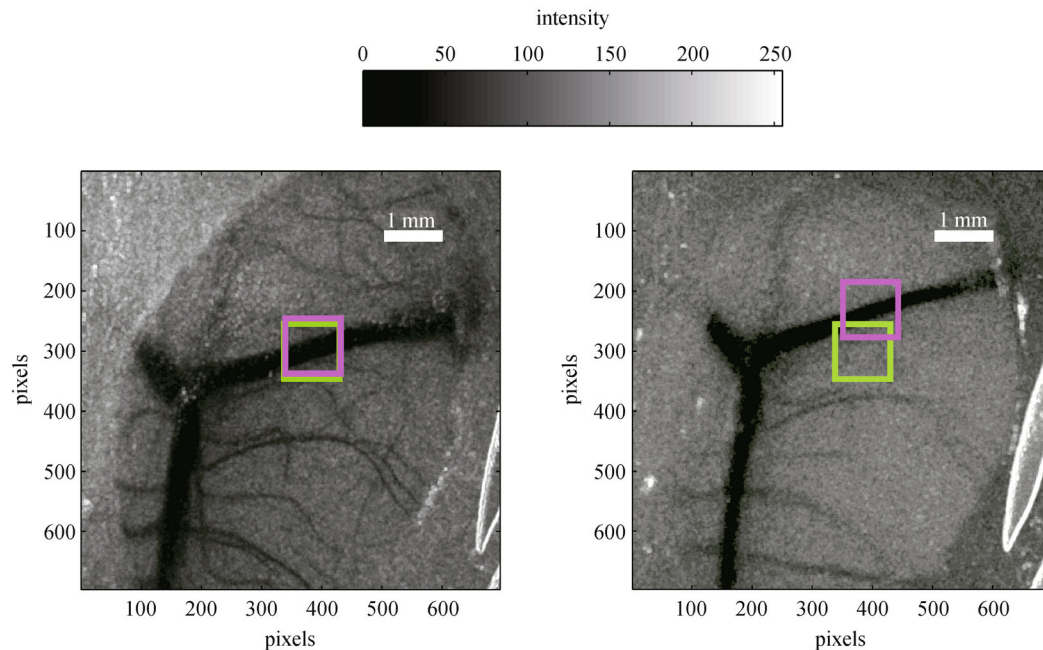
Fig. 3 Two consecutive frames of the time lapse measurements. Green block denotes statically overlaid ROI, whereas purple block is defined by correlation-based motion tracker
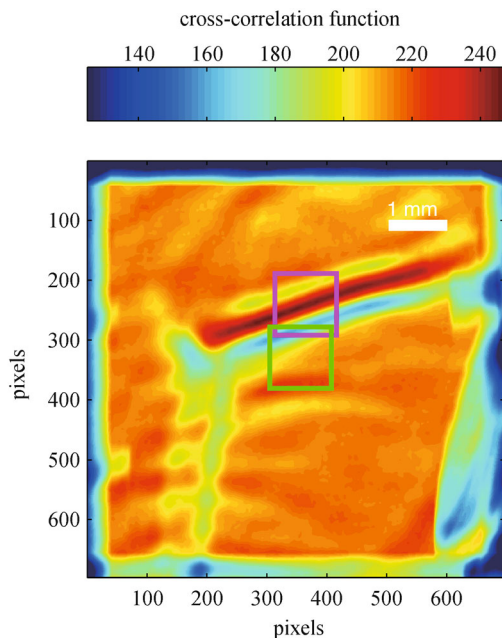

Fig. 4 Cross-correlations between selection and the next frame in series. Purple block shows new ROI coordinates with respect to maximum of cross-correlation function; green block is a statically overlaid ROI

sion is a key factor that leads to ischemic stroke development [28,29]. In 1959, Lassen proposed a concept for the retention of CBF even if arterial blood pressure dramatically changes from 60 to 150 mmHg [30]. How-

ever, changes in arterial pressure by even 10 mmHg are accompanied by the changes in CBF of 2%–7% [31]. Until now, research on the effects of changes of arterial pressure on CBF is insufficient. Hence, we performed a series of experiments with normotensive rats ($n = 10$) and hypertensive ($n = 10$) rats by phenylephrine. Phenylephrine is known to be unavailable over the blood-brain barrier [32], and thus we can measure the changes in CBF induced by the changes in blood pressure only. Arterial hypertension was provoked using the method described in Ref. [33]. According to this method, rats were kept in isolation or overpopulation for four months. Then, all rats were anesthetized using isoflurane, and craniotomy was performed using dental drill (Mikroton, Aesculap) with constant saline irrigation to prevent tissue overheating. CBF in rat cortex was measured at   30 min after surgery. Blood pressure monitoring was applied using pressure catheters (PE-50 with a PE-10 tip, Scientific Commodities Inc., Lake Havasu City, Arizona, USA) introduced into the femoral artery and the PowerLab data acquisition device.

Phenylephrine was injected at three time points to raise the peripheral blood pressure (PBP). Results of this study showed that phenylephrine injection leads to dose-dependent increase of blood pressure in normotensive rats from (105 ± 5) mmHg to (171 ± 7) mmHg (from (142 ± 9) mmHg to (195 ± 11) mmHg in hypertensive rats). The rate of change of blood pressure in normotensive rats (64%) was greater than that (37%) in hypertensive rats (Fig. 6(a)). This result can be explained by higher basal blood pressure level in hypertensive individuals.

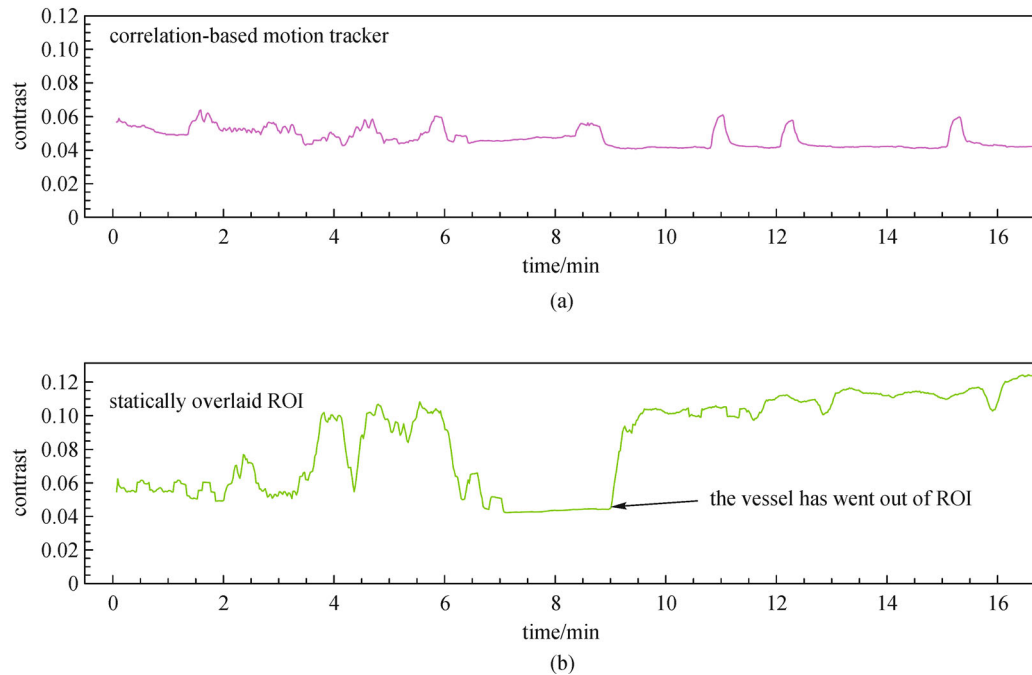Changes in CBF under rapidly increasing PBP were

Fig. 5   Results of time lapse measurements performed (a) with statically overlaid ROI and (b) with correlation based motion tracker

detected in hypertensive rats only. The typical dynamics of CBF in normotensive and hypertensive rats are shown in Figs. 6(b) and 6(c).

As shown in Fig. 6, an increase in CBF at microcirculatory level in response to sharp rise in peripheral arterial pressure is typical for hypertensive rats, rather than normotensive rats. CBF remains constant in normotensive rats, independent of significant hypertensive response to phenylephrine. In contrast to normotensive rats, in hypertensive individuals, peripheral pressure response to the third phenylephrine injection is accompanied by weak increase in microcirculatory and appreciable decrease in CBF in sagittal sinus. The possible mechanism underlying these processes is the decrease in venous blood flow, i.e., reallocation of CBF to the area where the blood–tissue oxygen exchange occurs, apparently, to prevent hypoxia. The method proposed for differentiation of blood flow at macro- and microlevels allows multi-scaled analysis of CBF at spasmodic changes in arterial pressure on the basis of chronic hypertension. Such kind of analysis is important particularly for further studies on hemorrhagic and ischemic stroke development provoked by hypertension.

4   Discussion and conclusion

The practical application of the proposed algorithm to study CBF in living animals shows that histogram analysis of an image obtained by LSCI may potentially improve the qualitative measurements of conventional LSCI. However, the advantages of this method over the other techniques

should be verified to improve method efficiency. A possible approach to implement is a detailed analysis of the contrast distribution involving calculations of skewness, kurtosis, and higher moments, which characterize the shape of the contrast distribution. The contrast distribution can be considered as a rough approximation to velocity distribution in the ROI. Such approximation seems to be inappropriate for quantitative estimation, but is still acceptable for comparative qualitative analysis. As such, kurtosis and dispersion properties of the velocity distribution can be used as a diagnostic variable as well as the most probable value used in this study. Asymmetry of the distribution (skewness) requires more complicated analysis. This property can be referred to sensitivity of experimental setup with specified settings (e.g., exposure time, f-number, and uniformity of illumination). In this case, averaging the contrast value over the entire ROI can provide inaccurate result that is biased to the stretched, asymmetric side tail of the contrast distribution. The possible resolution to this problem is analyzing the skewness of the contrast distribution for a sample with known parameters and considering the results of analysis in the subsequent measurements. We believe that the analysis of these properties may provide some additional information on micro- and macrocirculations and their temporal dynamics.

Animal study demonstrated that acute hypertensive responses induced by bolus injection of phenylephrine in three different doses have no effect on CBF in normotensive individuals. In hypertensive rats, the third injection of phenylephrine led to an increase in macrocirculation and a
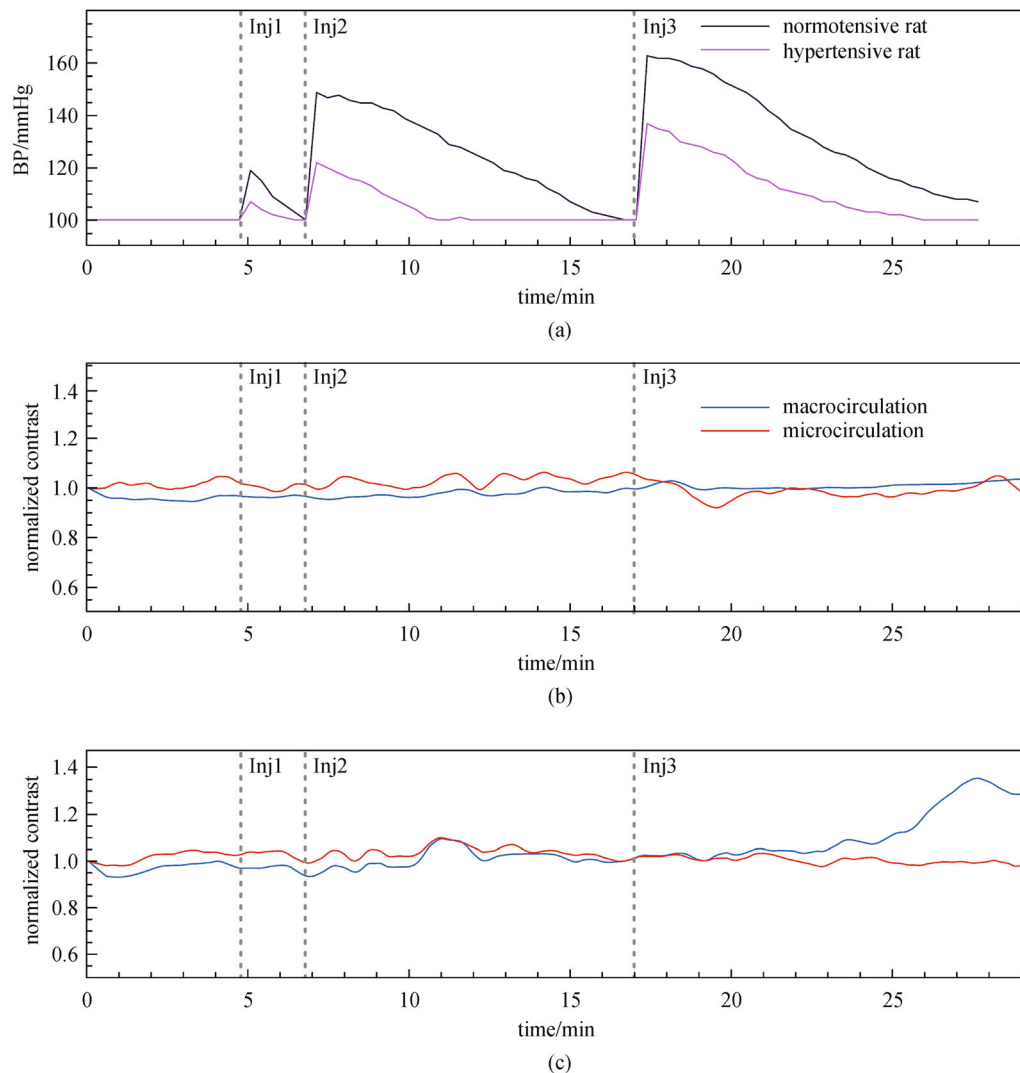
Fig. 6   Typical example of (a) changes of mean arterial pressure and CBF after bolus injection of phenylephrine in three doses (0.25, 0.5, and 1 μg/kg) in (b) normotensive and (c) hypertensive rats

decrease in microcirculation of CBF as response to dramatically increased PBP. Thus, the differentiation between macro- and microcirculations under functional activation allows for physiological analysis of the hemodynamic mechanisms underlying pathological changes in CBF, which in turn can help in developing new methods for pharmacological correction of macro- and microcirculation in the brain under different physiological conditions.

References

1. Fercher A F, Briers J D. Flow visualization by means of single-exposure speckle photography. Optics Communications, 1981, 37 (5): 326–330

2. Li P, Ni S, Zhang L, Zeng S, Luo Q. Imaging cerebral blood flow through the intact rat skull with temporal laser speckle imaging. Optics Letters, 2006, 31(12): 1824–1826

3. Luo Z, Yuan Z, Pan Y, Du C. Simultaneous imaging of cortical hemodynamics and blood oxygenation change during cerebral ischemia using dual-wavelength laser speckle contrast imaging. Optics Letters, 2009, 34(9): 1480–1482

4. Dunn A K. Laser speckle contrast imaging of cerebral blood flow. Annals of Biomedical Engineering, 2012, 40(2): 367–377

5. Parthasarathy A B, Weber E L, Richards L M, Fox D J, Dunn A K. Laser speckle contrast imaging of cerebral blood flow in humans during neurosurgery: a pilot clinical study. Journal of Biomedical Optics, 2010, 15(6): 066030

6. Briers J D. Laser doppler and time-varying speckle: a reconciliation. Journal of the Optical Society of America A, 1996, 13(2): 345–350

7. Boas D A, Dunn A K. Laser speckle contrast imaging in biomedical optics. Journal of Biomedical Optics, 2010, 15(1): 011109

8. Huang Y C, Ringold T L, Nelson J S, Choi B. Noninvasive blood flow imaging for real-time feedback during laser therapy of port wine stain birthmarks. Lasers in Surgery and Medicine, 2008, 40(3): 167–173

9. Tamaki Y, Araie M, Kawamoto E, Eguchi S, Fujii H. Noncontact, two-dimensional measurement of retinal microcirculation using laser speckle phenomenon. Investigative Ophthalmology & Visual Science, 1994, 35(11): 3825–3834

10. Sugiyama T, Mashima Y, Yoshioka Y, Oku H, Ikeda T. Effect of unoprostone on topographic and blood flow changes in the ischemic optic nerve head of rabbits. Archives of Ophthalmology, 2009, 127(4): 454–459

11. Wang J, Zhang Y, Xu T H, Luo Q M, Zhu D. An innovative transparent cranial window based on skull optical clearing. Laser Physics Letters, 2012, 9(6): 469–473

12. Miao P, Lu H, Liu Q, Li Y, Tong S. Laser speckle contrast imaging of cerebral blood flow in freely moving animals. Journal of Biomedical Optics, 2011, 16(9): 090502-1–090502-3

13. Dunn A K, Devor A, Bolay H, Andermann M L, Moskowitz M A, Dale A M, Boas D A. Simultaneous imaging of total cerebral hemoglobin concentration, oxygenation, and blood flow during functional activation. Optics Letters, 2003, 28(1): 28–30

14. Durduran T, Burnett M G, Yu G, Zhou C, Furuya D, Yodh A G, Detre J A, Greenberg J H. Spatiotemporal quantification of cerebral blood flow during functional activation in rat somatosensory cortex using laser-speckle flowmetry. Journal of Cerebral Blood Flow and Metabolism, 2004, 24(5): 518–525

15. Dunn A K, Bolay H, Moskowitz M A, Boas D A. Dynamic imaging of cerebral blood flow using laser speckle. Journal of Cerebral Blood Flow and Metabolism, 2001, 21(3): 195–201

16. http://web.stanford.edu/group/hopes/cgi-bin/wordpress/2012/04/neuroimaging/

17. Strong A J, Bezzina E L, Anderson P J, Boutelle M G, Hopwood S E, Dunn A K. Evaluation of laser speckle flowmetry for imaging cortical perfusion in experimental stroke studies: quantitation of perfusion and detection of peri-infarct depolarisations. Journal of Cerebral Blood Flow and Metabolism, 2006, 26(5): 645–653

18. Bandyopadhyay R, Gittings A S, Suh S S, Dixon P K, Durian D J. Speckle-visibility spectroscopy: a tool to study time-varying dynamics. Review of Scientific Instruments, 2005, 76(9): 093110

19. Davis M A, Kazmi S M, Dunn A K. Imaging depth and multiple scattering in laser speckle contrast imaging. Journal of Biomedical Optics, 2014, 19(8): 086001

20. Lemieux P A, Durian D J. Investigating non-Gaussian scattering processes by using nth-order intensity correlation functions. Journal of the Optical Society of America A, 1999, 16(7): 1651–1664

21. Duncan D D, Kirkpatrick S J. Can laser speckle flowmetry be made a quantitative tool? Journal of the Optical Society of America A, 2008, 25(8): 2088–2094

22. Ramirez-San-Juan J C, Ramos-García R, Guizar-Iturbide I, Martínez-Niconoff G, Choi B. Impact of velocity distribution assumption on simplified laser speckle imaging equation. Optics Express, 2008, 16(5): 3197–3203

23. Yuan S, Dunn A K, Boas D A. Calibration in laser speckle contrast imaging. In: Proceedings of Biomedical Topical Meeting Fort Lauderdale, Poster Session II (ME), 2006

24. Thompson O B, Andrews M K. Tissue perfusion measurements: multiple-exposure laser speckle analysis generates laser Doppler-like spectra. Journal of Biomedical Optics, 2010, 15(2): 027015

25. Domoki F, Zölei D, Oláh O, Tóth-Szuki V, Hopp B, Bari F, Smausz T. Evaluation of laser-speckle contrast image analysis techniques in the cortical microcirculation of piglets. Microvascular Research, 2012, 83(3): 311–317

26. Gonzalez R C, Woods R E. Digital Image Processing. New Jersey: Prentice Hall, 2002, 793

27. Tom W J, Ponticorvo A, Dunn A K. Efficient processing of laser speckle contrast images. IEEE Transactions on Medical Imaging, 2008, 27(12): 1728–1738

28. Qureshi A I. The importance of acute hypertensive response in ICH. Stroke, 2013, 44(6, Supplement 1): S67–S69

29. Qureshi A I. Acute hypertensive response in patients with stroke: pathophysiology and management. Circulation, 2008, 118(2): 176–187

30. Lassen N A. Cerebral blood flow and oxygen consumption in man. Physiological Reviews, 1959, 39(2): 183–238

31. Heistad D D, Kontos H A. Cerebral circulation. Comprehensive Physiology, 1983, 137–182

32. Olesen J. The effect of intracarotid epinephrine, norepinephrine, and angiotensin on the regional cerebral blood flow in man. Neurology, 1972, 22(9): 978–987

33. Semyachkina-Glushkovskaya O V, Lychagov V V, Bibikova O A, Semyachkin-Gluskovskiy I A, Sindeev S S, Zinchenko E M, Kassim M M, Braun H A, Al-Fatle F, Al Hassani L, Tuchin V V. The assessment of pathological changes in cerebral blood flow in hypertensive rats with stress-induced intracranial hemorrhage using Doppler OCT: particularities of arterial and venous alterations. Photonics and Lasers in Medicine, 2013, 2(2): 109–116
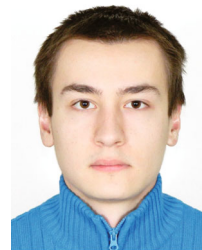
Arkady S. Abdurashitov graduated from high school №3 of Saratov. In present time, he is a student of National Research Saratov State University. He is the winner of the Student Scientific Conference, National Research Saratov State University, 2014 and participated in the poster session of Saratov Fall Meeting 2014 conference. His fields of interest are optics, physics, programming, data processing, data visualization.

Vladislav V. Lychagov received his M.S. degree in Physics in 2003 and Ph.D. degree in Optics in 2007, both from Saratov State University, Russia. Since that time, he obtained his postdoctoral training in Optics and Biophotonics department of Saratov State University. Since 2010, he is research associate professor of Optics and Biophotonics department. His research interests include wave and coherent optics, coherent imaging and microscopy, interferometric measurements and data processing.

Olga A. Sindeeva received her M.S. degree in Biology (diploma with excellence) in 2012 from Saratov State University, Russia. Since that time, she is a Ph.D. student in Saratov State University, Biological department, Chair of Physiology Human and Animals. Since 2014, she is research associate of Biological department. Her research interests include stress-induced vascular diseases, such as: stroke at different ages and sexes, hypertension, gastric ulcer; stress-limiting system, early indicators of vascular complications.

Oxana V. Semaychkina-Glushkovskaya received her M.Sc. equivalent in Physiology (diploma with excellence) in 1999, and Ph. D. equivalent in Biological Sciences in 2002, both from Saratov State University, Russia. From 2002 to 2013, she was an Assistant of Professor (2002 – 2007), Associate Professor (2007 – 2012), Professor (2012 – 2013) in Saratov State University, Department of Biology, Chair of Physiology Human and Animals. Since 2013, she is Head of Chair of Physiology of Human and Animals, Department of Biology, Saratov State University. Her research interests include stress-induced vascular damages, stress-limiting system, early indicators of vascular complications, mechanisms underlying neonatal stroke, transformation of peptic ulcer to cancer, role of sex hormones in stress-resistance and stress-reactivity of vascular system, development new animal models: stress-induced neonatal stroke, stress-related peptic ulcer and gastric cancer, technologies for a prognosis of stress-related vascular "catastrophes" such as stroke and ulcer bleeding.

Valery V. Tuchin received a M.S. degree in Radio-Physics and Electronics (1966), a Ph. D. degree in Optics (1974), and a DrSc in Laser Physics (1982) from Saratov State University, Saratov, Russia. Currently, he is a Professor and holds the Chair of Optics and Biophotonics of Saratov State University. He is also a Director of the Research-Educational Institute of Optics and Biophotonics at Saratov State University and Head of Laboratory on Laser Diagnostics of Technical and Living Systems, Inst. of Precise Mechanics and Control, RAS. His research interests include biophotonics, tissue optics, laser medicine, tissue optical clearing, and nanobiophotonics. He has authored more than 350 peer-reviewed papers, handbooks, monographs, text books, tutorials, and book chapters, holder of more than 50 patents. He is a member of SPIE, OSA, and IEEE. He is a fellow of SPIE and has been awarded Honored Science Worker of the Russia (1999), SPIE Educator Award (2007), FiDiPro (Finland) (2011), and Chime Bell Prize of Hubei Province, China (2014).